Inorg. Chem. **2007**, *46*, 7371–7377

Synthesis and Structural Characterization of a New Nanoporous-like Keggin Heteropolyanion Salt: $K_3(H_2O)_4[H_2SiVW_{11}O_{40}](H_2O)_{8+x}$

Rodrigo de Paiva Floro Bonfim,[†] Luiza Cristina de Moura,[†] Hélène Pizzala,[‡] Stefano Caldarelli,[‡] Sébastien Paul,[§] Jean Guillaume Eon,*[,†] Olivier Mentré,[§] Mickaël Capron,[§] Laurent Delevoye,[§] and Edmond Payen[§]

Instituto de Química, Universidade Federal do Rio de Janeiro, Brazil, JE 2421 TRACES, Université d'Aix Marseille, Campus Saint Jérôme 13013 Marseille, France, and Unité de Catalyse et de Chimie du Solide, UMR-CNRS-8181, U S T Lille, France

Received February 28, 2007

Single crystals of the potassium salt $K_3(H_2O)_4[H_2SiVW_{11}O_{40}](H_2O)_{8+x}$ of the vanadium monosubstituted α-Keggin dodecatunsgstosilicate were grown from an aqueous solution and analyzed by EDS, XRD, vibration and electronic spectroscopy, and ^1H, ^{51}V, and ^{29}Si solid-state NMR spectroscopy. Results indicate the formation of a nanoporous-like compound of hexagonal symmetry (space group $P6_2$) with large, water-filled channels running along the *c* axis. A uniform distribution of vanadium over the 12 metal sites of the α-Keggin anion is observed by XRD. Two different neighborhoods were characterized by ^{51}V NMR in a 2:1 ratio ($\delta_{iso} = -546.3$ and -536.2 ppm), in accordance with a difference in the number of potassium ions in the second coordination shell of vanadium.

Introduction

A substantial amount of work has been performed in the last 30 years to prepare and characterize substituted Keggin polyoxotungstate species in solution.[1,2] In contrast, few studies have been devoted to solid-state characterization and, in particular, to single crystal analysis.[3,4] In view of our interest in polymetallic polyanions as precursors or catalysts for heterogeneous oxidation reactions,[2] we have started a systematic investigation of the synthesis and structure of the corresponding alkaline salts.

The most-studied polyoxotungstate anions have the Keggin structure with formula $[XW_{12}O_{40}]^{n-}$, where X is a tetrahedral heteroatom ($X = Si^{IV}$, Ge^{IV}, P^V, or As^V). The nonlacunary α-Keggin structure is composed of four equivalent W_3O_{13} triads, which consist of three edge-sharing octahedra linked to the XO_4 central tetrahedron. These triads are connected to each other via corner-sharing of WO_6 octahedra, leading to an overall symmetry T_d. The β isomer is obtained by the rotation of one W_3O_{13} group by 60° (overall C_{3v} symmetry) and the γ isomer by the rotation of two groups (overall C_{2v} symmetry).[5] The monolacunary α-Keggin ion resulting from the loss of one WO_6 octahedron (C_1 symmetry) was also characterized by X-ray diffraction (XRD) as single crystal.[6] Filling the void in the monolacunary α-Keggin polyoxotungstate anion with vanadium in a different oxidation state enabled to prepare salts of the mixed polyoxoanions $[PV^{IV}M_{11}O_{40}]^{n-}$, $[PV^{V}M_{11}O_{40}]^{n-}$, $[SiV^{IV}M_{11}O_{40}]^{n-}$, and $[SiV^{V}M_{11}O_{40}]^{n}$ (M = Mo or W).[7] However, the authors report that only the method based on the use of the vanadyl ion could be reproduced. Single crystals of the salt $[(n\text{-}C_4H_9)_4N]_4[PVW_{11}O_{40}]$ were recently prepared following the same protocols; these crystals and powders of the potassium salt were studied by ^{51}V solid-state magic-angle spinning (MAS) NMR spectroscopy.[8]

In this work, we report a new preparation method for the potassium salt of the monosubstituted α-Keggin tungstosili-

* To whom correspondence should be addressed. E-mail: jgeon@iq.ufrj.br. Phone: 55-21-2562-7819. Fax: 55-21-2562-7559.
[†] Universidade Federal do Rio de Janeiro.
[‡] Université d'Aix Marseille.
[§] Unité de Catalyse et de Chimie du Solide.

(1) Pope, M. T. *Heteropoly and Isopoly Oxometalates*; Springer-Verlag. New York, 1983.
(2) (a) Korhevnikov, I. V. *Chem. Rev.* **1998**, *98*, 171−198. (b) Mizuno, N.; Misono, M. *Ibid.* **1998**, *98*, 199−217. (c) Katsoulis, D. E., *Ibid.* **1998**, *98*, 359−387.
(3) França, K. M. C.; Eon, J. G.; Fournier, M.; Payen, E.; Mentré, O. *Solid State Sci.* **2005**, *7*, 1533−1541.
(4) Leparulo-Loflus, M. A.; Pope, M. T. *Inorg. Chem.* **1987**, *26* (13), 2112−2120.
(5) Tézé, A.; Hervé, G. *Inorganic Syntheses*; Wiley & Sons: New York, 1990; Vol. 27.
(6) Matsumoto, K.; Sasaki, Y. *Bull. Chem. Soc. Jpn.* **1976**, *49*, 156−158.
(7) Domaille, P. J. *J. Am. Chem. Soc.* **1984**, *106*, 7677−7687.
(8) Huang, W.; Todaro, L.; Yap, G. P. A.; Beer, R.; Francesconi, L. C.; Polenova, T. *J. Am. Chem. Soc.* **2004**, *126*, 11564−11573.

10.1021/ic700384m CCC: $37.00
Published on Web 08/10/2007

cate $K_3(H_2O)_4[H_2SiVW_{11}O_{40}](H_2O)_{8+x}$. This compound was obtained by the addition of vanadate ion to the monolacunary α-Keggin polyoxotungstate; the synthesis was perfectly reproducible and allowed for the preparation of single crystals that could be analyzed by XRD and spectroscopic techniques. We have found that the secondary, nanoporous-like structure of the title compound is isomorphic to that described by Gao et al.[9] in salts of pure Keggin molybdosilicate and tungstosilicate. There is obviously great interest in investigating new polyanion-based nanoporous materials. The results presented here provide new insights regarding the conditions of synthesis and the stability of such compounds.

Experimental Section

Synthesis. Synthesis of the title compound was performed in an aqueous solution at pH 5.8 ± 0.09 using a Titrino 799 Potentiometric Titulation apparatus from Metrohm in the static pH titulation mode. The lacunary $K_8[\alpha\text{-}SiW_{11}O_{39}]$ was obtained following Tézé and Hervé;[5] Na_3VO_4 (98%, Sigma) and KCl (99%, Spectrum) were used as received. In 45 mL of hot H_2O, 3.8654 g (1.2 mmols) of $K_8[\alpha\text{-}SiW_{11}O_{39}]$ were dissolved under stirring. After cooling, the pH of the solution was adjusted to 5.8 with a 0.5 M HCl solution. A 45 mL solution of 0.1470 g (1.2 mmols) $NaVO_3$ was slowly added under stirring, while the pH was controlled to 5.8 with a 0.5 M HCl solution. After addition, the solution was stirred for 5 min. Next, the pH was adjusted to 2.0 using a 1M HCl solution and left under stirring at this same controlled value for 45 min. Then, 3 g (40 mmols) of KCl were added, and the volume of the solution was slowly reduced to half of its value. Yellow crystals were formed after the solution sat for 24 h, which were recristallized in hot water.

Elemental Analysis. The energy-dispersive spectroscopy (EDS) analysis has been performed on single crystals of the title compound using a JSM 5300 scanning electron microscope equipped with a PGT digital spectrometer. WO_3, V_2O_5, KCl, and SiO_2 pellets have been used as standards. Strongly homogeneous results were obtained at several points of different crystals. The average analysis leads to the ratio V/W/K/Si = 0.6:11:2.90:1.20, which is in good agreement with the expected 1:11:3:1 ratio, considering the semiquantitative approach of the experimental procedure.

Single-Crystal X-ray Diffraction Analysis. Because of the easy loss of weakly bound water molecules at ambient atmosphere and the subsequent collapse of crystals, a single crystal was protected by epoxy resin. The X-ray diffraction (XRD) data have been collected at 100 K on a Bruker X8 (Apex 2 area detector) equipped with an Oxford Cryostream cooling system. Data collection is reported in Table 1 with crystal and refinement characteristics. The intensities have been integrated from the collected frames and corrected for background, Lorentz, and polarization effects, using *SAINT*,[10] and *SADABS* software was used for crystal/detector area absorption.[11] The lattice parameters have been refined from the complete data set. The systematic extinctions show the existence of a 3_1 or 6_2 screw axis. The refinement satisfactorily converged in the asymmetric $P3_121$ or $P6_2$ space groups; however, the more-symmetric latter has been selected because of the smaller number of refined parameters and the better values of the reliability factors. The six independent metal positions have been determined by direct methods using *SHELXS* and refined using *SHELXL*, included in the *SHELTXL* package.[12] The additional potassium, silicon, and oxygen atoms have been located through the Fourier difference syntheses calculations. Anisotropic thermal parameters have been considered for cations only. The particular features of the refinement are listed below:

(i) For the six metal positions, a V/W ratio close to 1:11 has been refined. It shows both good agreement with the expected $SiVW_{11}O_{40}$ formulation and a complete V/W statistic occupancy due to the rotational disorder of the Keggin anion in the crystal framework. V/W occupancies have been finally restrained equally for the six sites, leading to W/V occupancies 0.911(6)/0.089(6) = 10.93, W: 1.07, V.

(ii) The cohesion between superimposed HPAs along the *c* axis is performed by $K2_a$ and $K2_b$ that half-occupy two close positions (separation 1.46 Å), identically coordinated by $OH2_1$ and $OH2_2$.

(iii) The occupancies of water molecules in the channels (description below) have also been restrained to be half-

Table 1. Crystal and Refinement Data

$K_3(H_2O)_4[H_2SiV_1W_{11}O_{40}](H_2O)_{8+x}$	
cryst data (T = 100 K)	
symmetry	hexagonal
space group	$P6_2$ (no. 171)
unit cell (Å)	a = 18.8901(1)
	c = 12.4857(2)
	V = 3858.44(7) Å^3
Z	3
Data collection	
equipment	Bruker X8, Apex2 area detector
λ (Mo Kα (graphite monochromator)) (Å)	0.7107
D_{calcd}	3.97 g/cm^3
color	yellow
scan mode	ω and φ scans
Θ min-max (deg)	2.05−25.41
μ (mm^{-1})(for λ, Kα = 0.7107 Å)	25.03
T_{min}/T_{max}	0.395
R(int) (%)	6.86
recording reciprocal space	$-22 \le h, k \le 22$, $-15 \le l \le 15$
number of measured reflns	31 394
N indep. reflns ($I > 2\sigma(I)$), total	4747/4598
cryst dimensions (mm)	0.3 × 0.3 × 0.4
Refinement	
number of refined params	201
refinement method, program	L.S. on I, *SHELXL*
R1(F) [$I > 2\sigma I$]/R1(F) [all data], %	3.35/3.49
wR2(F^2) [$I > 2\sigma I$]/wR2(F^2) [all data], %	8.50/8.47
$w = 1/(\sigma^2(F_0^2)+(0.038*P)^2+78*P)$ with $P = (\text{Max}(F_0^2,0) + 2*F_c^2)/3$	
GOF	1.073
max/min resid. elect. density (e$^-$/Å^3)	1.51/−1.48
reflns extinction coefficient	0.00038(3)

(9) Gao, S.; Cao, R.; Bi, W.; Li, X.; Lin, Z. *Microporous Mesoporous Mater.* **2005**, *80*, 139−145.
(10) *SAINT 7*; Bruker Analytical X-ray Systems: Madison, WI, 2000.
(11) *SADABS: Area-Detector Absorption Correction*; Siemens Industrial Automation, Inc.: Madison, WI, 1996.
(12) *SHELXTL package*; Bruker Analytical X-ray Systems: Madison, WI, 1997.

Table 2. Pertinent Distances (Angstroms)

M1−		M2−		M3−		M4−		M5−		M6−	
O8	1.70(1)	O18	1.69(1)	O6	1.70(1)	O11	1.69(1)	O4	1.68(1)	O16	1.70(1)
O20	1.90(1)	O12	1.89(1)	O17	1.89(1)	O15	1.89(1)	O15	1.89(1)	O12	1.89(1)
O7	1.90(1)	O7	1.91(1)	O9	1.91(1)	O1	1.90(1)	O9	1.91(1)	O20	1.90(1)
O1	1.93(1)	O5	1.91(1)	O3	1.93(1)	O17	1.90(1)	O13	1.91(1)	O3	1.92(1)
O5	1.93(1)	O10	1.92(1)	O14	1.95(1)	O10	1.92(1)	O14	1.92(1)	O13	1.92(1)
O2	2.35(1)	O 2	2.33(1)	O19	2.36(1)	O2	2.35(1)	O19	2.33(1)	O19	2.34(1)
Si−		M−M e.s.		M−M c.s.		K1−		K2a−		K2b−	
O19	1.61(1)	M1−M2	3.344(1)	M1−M2	3.683(1)	O18	2.67(1)	OH22	2.68(1)	OH21	2.68(1)
O19	1.61(1)	M1−M4	3.362(1)	M1−M6	3.680(1)	O4	2.68(1)	OH22	2.68(1)	OH21	2.68(1)
O2	1.61(1)	M2−M4	3.345(1)	M2−M6	3.667(1)	O10	2.78(1)	OH21	2.76(1)	OH22	2.76(1)
O2	1.61(1)	M3−M5	3.345(1)	M3−M4	3.685(1)	O13	2.79(1)	OH21	2.76(1)	OH22	2.76(1)
		M3−M6	3.364(1)	M3−M5	3.687(1)	OH22	2.85(1)	O7	2.98(2)	O9	2.98(2)
		M5−M6	3.348(1)	M4−M5	3.673(1)	OH21	2.86(1)	O7	2.98(2)	O9	2.98(2)
						O4	3.09(1)	O5	3.00(1)	O14	2.99(2)
						O18	3.10(1)	O5	3.00(1)	O14	2.99(2)

occupied due to short O−O distances and to large thermal parameters. It shows a certain degree of disorder. As a matter of fact, a number of residual electronic density peaks subsist in the tunnels but do not match additional oxygen atoms. It is legitimate to suspect extra nonstructural *zeolitic* water from the thermogravimetric analysis, as discussed below. However, the crystal structure refinement formally leads to the nominal $K_3[H_2SiV_1W_{11}O_{40}]\ (H_2O)_{12}$ formula.

The final $R1_{obs(I>2\sigma(I))}$ was of 3.35%. The pertinent distances are reported in the Table 2. Atomic coordinates and anisotropic displacement parameters are available as Supporting Information.

Vibration Spectroscopy. Infrared spectra were recorded using CsI pellets in the mid region (4000−400 cm^{-1}) and in the far region (600−200 cm^{-1}) on a 550 FTIR Nicolet spectrometer. Raman spectra were acquired in the range of 100−1200 cm^{-1} with a Raman LabRAM Infinity microprobe (Jobin Yvon) equipped with a liquid-nitrogen-cooled detector and a frequency-doubled Nd:YAG laser supplying the excitation line at 632 nm. The power was less than 5mW at the sample.

Electronic Spectroscopy. UV-vis diffuse reflectance spectra were acquired in the range of 200−800 nm on a Varian Cary 5 spectrometer equipped with a Harrick diffuse reflectance attachment with praying mantis geometry.

Solid-State NMR Analysis. The ^1H and ^{51}V magic-angle spinning (MAS) NMR experiments were carried out on a Bruker AV400 (9.4 T) spectrometer operating at Larmor frequencies of 400.13 and 105.2 MHz, respectively, using a 2.5 mm MAS probehead. The ^1H MAS NMR spectrum was recorded with a single-pulse acquisition with a $\pi/2$ pulse angle and a recycle delay of 15 s. The spinning rate was set to 17 kHz. The ^1H spectrum was referenced at 4.8 ppm, relative to H_2O. The ^{51}V MAS NMR spectra were recorded using a single-pulse acquisition with a $\pi/12$ small pulse angle and a recycle delay of 3 s. Two spinning rates (20 and 28 kHz) were used to determine the isotropic chemical shift of the central transition. The ^{51}V chemical shifts were referenced with respect to the crystalline V_2O_5 used as an external standard. ^{29}Si MAS NMR experiments were carried out on a Bruker AV100 (2.35 T) spectrometer operating at ^{29}Si Larmor frequencies of 19.9 MHz, using a 7 mm MAS probehead. The ^{29}Si MAS NMR spectra were recorded at a 5 kHz spinning rate, using a $\pi/10$ single-pulse excitation with a recycle delay of 10 s, to prevent saturation. ^{29}Si chemical shifts were referenced with respect to $Si(CH_3)_4$, used as an external standard.

Results and Discussion

Vibration Spectroscopy. Figure 1 and Table 3 present the infrared and Raman spectra of the title compound with their assignments, respectively. The infrared bands can be attributed to an α- or *β*-Keggin structure, in accordance with the literature, as follows: 981 cm^{-1} (ν_{as} W−O_d), 924 cm^{-1} (ν_{as} Si−O_a), 894 cm^{-1} and 878 cm^{-1} (ν_{as} W−O_b−W), 781 cm^{-1} (ν_{as} W−O_c−W).[13,14] Spectral differences between α and *β* isomers occur specifically in the low-frequency region, in the 400−300 cm^{-1} range. The spectra of the α isomers generally exhibit a strong and sharp band around 370−380 cm^{-1} and a medium or weak band at around 340 cm^{-1}, which can be considered as a characteristic of the α form.[14] Thus, the two bands observed at 377 and 335 cm^{-1} indicate the formation of a polyoxoanion with the α-Keggin structure. The following assignments of the Raman spectrum can be made. Two strong bands at 997 and 991 cm^{-1} are attributed to symmetric and asymmetric stretching ν_s (W−O_d) ν_{as} (W−O_d), respectively. Weak bands are also observed at 899 cm^{-1} (ν_{as}, W−O_b−W) and 544 cm^{-1} (ν_s, W−O_c−W). The ν_s (W−O_a) band at 220 cm^{-1} is characteristic of the α isomer.[14]

Electronic Spectroscopy. The title compound presents a wide absorption band in the UV, with absorption edge in the visible region around 500 nm, as shown in Figure 2. Because the lacunary SiW_9 and SiW_{11} compounds as well as the pure SiW_{12} α-Keggin compounds display O → W ligand-to-metal charge transfer bands in the range of 200−400 nm, the observed absorption in the visible spectrum was attributed to vanadium; the value of the absorption edge is in agreement with octahedral coordination.[15]

Crystal Structure Description. The structure is built on the well-known α-Keggin HPAs interconnected by ionic and hydrogen bonds. Within the anions, each metal is off-

(13) Rocchiccioli-Deltcheff, C.; Fournier, M.; Franck, R. *Inorg. Chem.* **1983**, *22* (2), 207−216.
(14) Thouvenot, R.; Fournier, M.; Franck, R.; Rocchiccioli-Deltcheff, C. *Inorg. Chem.* **1984**, *23* (5), 598−605.
(15) Eon, J. G.; Olivier, R.; Volta, J. C. *J. Catal.* **1994**, *145*, 318−326.

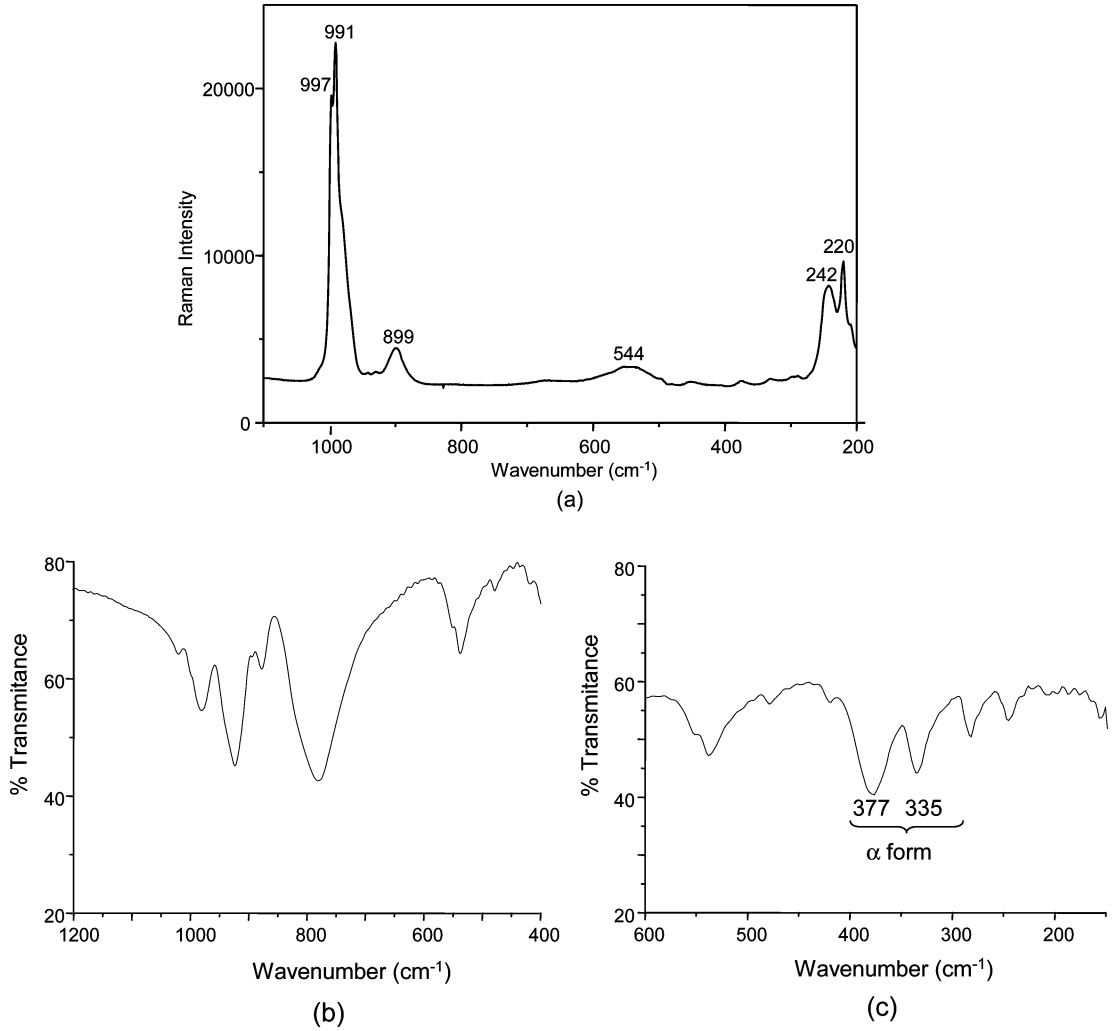

Figure 1. Raman (a) and infrared (b) and (c) spectra of $K_3(H_2O)_4[H_2SiV_1W_{11}O_{40}]\cdot 9.5H_2O$.

Table 3. Assignments in the Vibration Spectra of Potassium Salt $K_3(H_2O)_4[H_2SiVW_{11}O_{40}](H_2O)_{8+x}$

α-$SiVW_{11}$			
IR		RAMAN	
1015 (w)[a]			
998 (sh)	ν_s (W−O_d)	997	ν_s (W−O_d)
981 (s)	ν_{as} (W−O_d)	991	ν_{as} (W−O_d)
924 (vs)	ν_{as} (Si−O_a)	899	ν_s (W−O_b−W)
894 (sh)	ν_{as} (W−O_b−W)		
878 (m)	ν_{as} (W−O_b−W)		
781 (vs)	ν_{as} (W−O_c−W)		
550 (sh)			
537 (m)		544	ν_s (W−O_c−W)
478 (w)			
419 (w)			
377 (s)	O_d−W−O_c		
335 (s)			
282 (m)			
245		242	
		220	ν_s (W−O_a)

[a] sh = shoulder, w = weak, m = medium, s = strong, and vs = very strong.

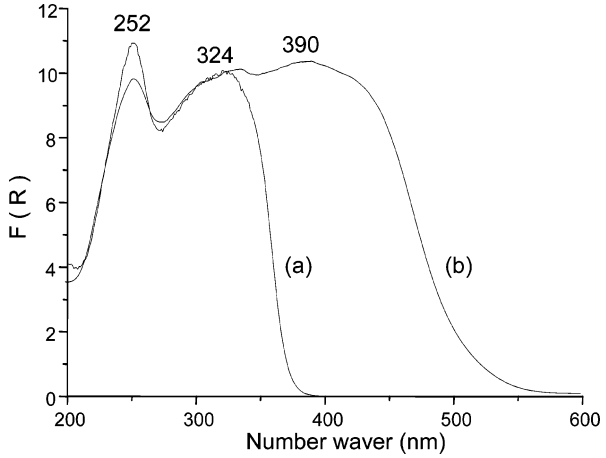

Figure 2. Diffuse-reflectance UV−vis spectra of $K_3(H_2O)_4[H_2SiV_1W_{11}O_{40}]\cdot 9.5\ H_2O$.

centered in a distorted O6 octahedron toward the external corner. Then, three octahedra share edges to form M_3O_{13} units. Four of them share corners to form the Keggin cages centered by the SiO_4 tetrahedron. Each metal is connected to one terminal oxygen through short bonds (1.68(1)−1.70(1) Å), four μ_2-bridging oxygen atoms with distances in the range of 1.89(1)−1.95(1) Å, and one μ_4-bridging oxygen (2.33(1)−2.36(1) Å). The HPAs are arranged as shown in part a of Figure 3 and form large channels with a radius of ∼11.5 Å, estimated from the bordering oxygen separations. The periphery of the channels can be viewed as a double helix of HPAs arranged together with respect to the $P6_2$ symmetry,

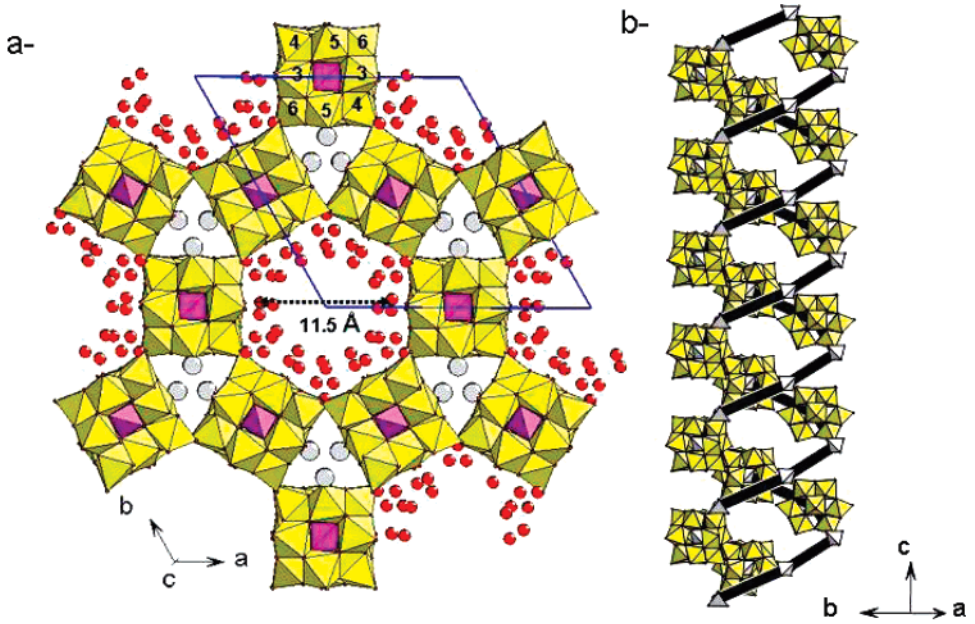

Figure 3. a- Arrangement of the HPAs, showing large nanoporous channels occupied by water molecules and the triangular channels gilled by K^+. b- Double helix of $[SiV_1W_{11}O_{40}H_2]^{3-}$ running along the 6-fold axis.

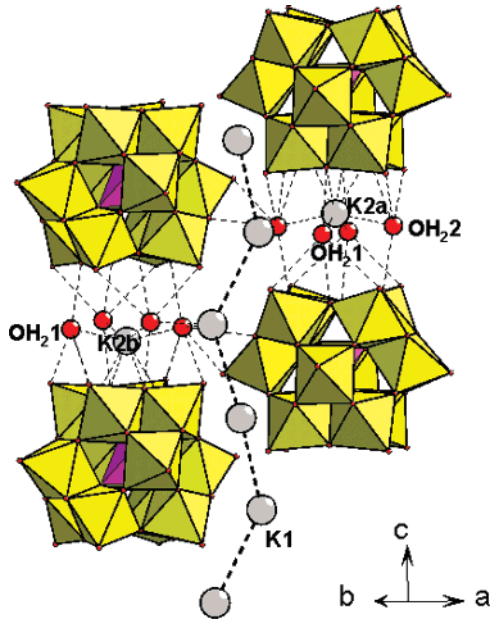

Figure 4. Anion packing along *c* showing the ionic and hydrogen bonds formed by $K2_{a/b}$ and $H_2O_{1/2}$ in broken lines.

as shown in part b of Figure 3. The separation between two subsequent anions on the same helix is 10.321(3) Å. This nanoporous-like crystal structure has been recently reported for $K_2(H_2O)_4H_2SiMo_{12}O_{40}\cdot 7H_2O$ and $K_2Na_2(H_2O)_4SiW_{12}O_{40}\cdot 4H_2O$.[9] However, in their work, Gao et al. reported the $P3_221$ space group for instance, leading to the refinement of some water molecules and sodium ions in positions $x = \sim 0.5$, $y = \sim 0$, z. Our choice of the more-symmetrical $P6_2$ space group alleviates this problem because it leads to a special 3(b) $^1/_2$, 0, z occupied by $K2_a$ and $K2_b$. K1 is surrounded by two water molecules and six oxygen corners from four individual HPAs, as shown in Figure 4. They form the triangular channels that alternate with anions and strongly hold the microporous tunnel walls. These are lined with 12 water molecules

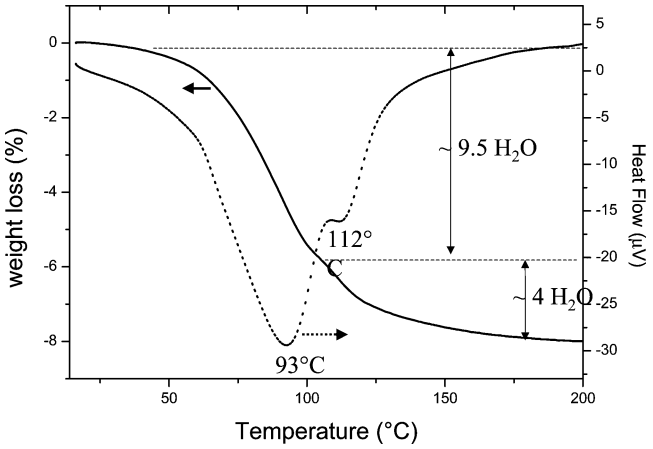

Figure 5. Differential thermal analysis and TGA plots for $K_3(H_2O)_4[H_2SiV_1W_{11}O_{40}]\cdot 9.5H_2O$.

observed from XRD. However the thermogravimetric analysis (TGA) plot shown in Figure 5 indicates a weight loss of ~8%, in better agreement with approximately 13.7 water molecules, including 1.7 zeolithic water molecules. Two consecutive endothermic phenomena are observed on the differential thermal analysis plot at 93 and 112 °C. The corresponding shoulder on the TGA plot delimits two subsequent water-loss stages: removal of the channel water and then the removal of the structural water. After thermal treatment up to 600 °C, the XRD powder pattern leads to the identification of only a $K_2W_4O_{13}$-like compound.[16] To fit our initial stoichiometry, we must suggest a deficient character for potassium already described in this structure[17] and the possible substitution of vanadium for tungsten.

As mentioned in the Introduction, the secondary, nanoporous-like structure of the title compound is isomorphic to

(16) $K_2W_4O_{13}$, ref 70−1229 of the JCPDS-ICDD file.
(17) Okada, K.; Marumo, F.; Iwai, S. I. *Acta Crystallogr.* **1978**, *B34*, 3193−3195.

that described by Gao et al.[9] Quite interestingly, these authors quote that the novel SiW_{12}-based compound could only be obtained when vanadium is introduced during the synthesis, together with tungsten in a V/W ratio of 1:20. The authors also comment that they obtained yellow crystals but failed to identify the presence of vanadium in the compound. From the chemical point of view, however, the announced conditions of synthesis and yellow color of the compound clearly suggest the possible formation of the monosubstituted Keggin polyoxometalate $SiVW_{11}$ as an impurity. It should be emphasized that the specific formation of a definite polyoxotungstate species cannot be granted when starting from vanadate and tungstate salts NH_4VO_3 and $Na_2WO_4{\cdot}2H_2O$ in an aqueous solution. On the other hand, the new synthesis described in this article starts from the monolacunary undodecatungstosilicate, whose intermediate was well characterized by vibration spectroscopy. Addition of vanadium to the structure resulted in the formation of the nonlacunary mixed-Keggin anion, as discussed above, which clearly indicates the stoichiometric insertion of vanadium in the lacunary Keggin SiW_{11} during synthesis.

Astonishingly, to our knowledge, only one study dealing with solids containing $[PV_nW_{12-n}O_{40}]^{(3+n)-}$ vanadium-substituted Keggin polytungstate has been reported so far.[8] In this work, the experimental difficulty in growing single crystals is clearly established, whereas microcrystalline powders are consistently formed. However, it has been possible to prepare compounds and analyze their crystal structures for $n = 1$ and 2 terms, using an excess of organic countercation n-$(C_4H_9)_4N^+$ or ethanol solvent. In the three presented crystal structures, the HPAs are isolated in positions created by the organic countercation packing, and no spectacular metallic sublattices are formed. Vanadium/tungsten atoms display positional disorder within the polymetallic clusters. In the case of a central silicon atom, one should also mention the $(TBA)_5SiW_{11}VO_{40}{\cdot}1.5H_2O$ reported by Salete et al.[18] and referenced as a private communication, while no crystal data are available. Finally, to be exhaustive, note the preparation of the Baker−Figgis dodecametalate $[PV_2W_{10}O_{40}]$, which has been crystallographically characterized in its cesium salt but shows a strong structural difference compared to the title Keggin anion, because the two V^{4+} cations adopt a square-pyramidal environment and share an edge.[19]

NMR Spectroscopy. Figures 6 and 7 present the ^1H and ^{51}V MAS spectra of the solid. The spectra were simulated using the DMfit program[20] developed by Massiot et al. Table 4 summarizes the isotropic and anisotropic chemical shifts and the quadrupolar parameters deduced from the deconvolution of the ^{51}V spectra. It is composed of two main lines at −546.3 and −536.2 ppm and their spinning side bands.

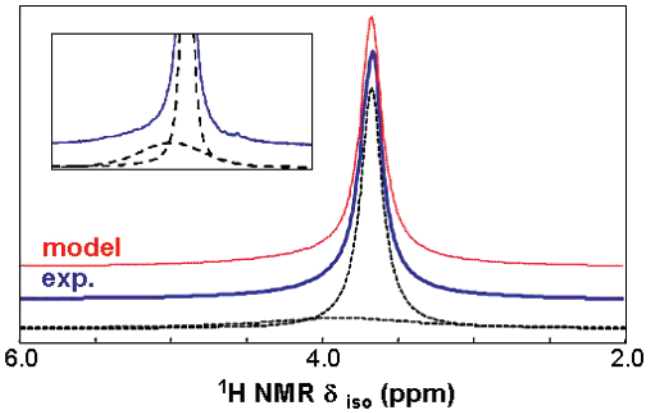

Figure 6. ^1H NMR spectrum of $K_3(H_2O)_4[H_2SiV_1W_{11}O_{40}]{\cdot}9.5H_2O$.

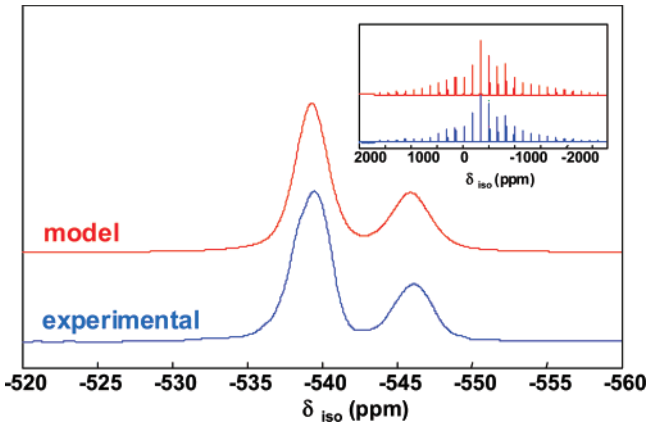

Figure 7. Central transition of the ^{51}V MAS NMR spectra obtained for the $SiVW_{11}O_{40}$ polyanion. The inset presents the full spectra with the spinning side bands.

Table 4. Chemical Shift, Quadrupolar Parameters and Relative Proportions Obtained after Modeling the Spectra of Figures 6 and 7

^1H	δ_{iso} (ppm)	fwhm (Hz)	relative percentage		
Site 1	3.68	74	∼74		
Site 2	3.88	1360	∼26		
^{51}V	δ_{iso} (ppm)	C_Q (MHz)	CSA (ppm)	η_{CS}	relative percentage
Site 1	−536.2	3.1	361	0.0	∼68
Site 2	−546.3	1.4	247	0.2	∼32

For comparison, a single peak is observed in an aqueous solution, around −548.5 ppm, in agreement with the literature.[4] The relative intensities of the two sites are equal to 32/68, taking into account the whole spectrum, that is, the central and spinning side bands. On the basis of the crystal structure, the observed ^{51}V NMR doublet can be assigned to two kinds of V/W sites from the fine observation of their second-neighbor shell. Indeed, V2 and V5 have three neighboring potassium ions with $d_{V-K} < 4.2$ Å, whereas V1, V3, V4, and V6 show a single potassium neighboring cation. In fact, it appears in Figure 1 that the former group borders the potassium-filled triangular channels, whereas the second group forms the walls of the porous water-filled tunnels. The quadrupolar parameters seem to reflect the structural role of each group. This distinction by itself involves drastic local differences. As a matter of fact, the theoretical 1:3−2:3 ratio between the two groups is well pictured by our refinement. It has been shown that, in Keggin heteropolyanions, the

(18) Salete, M.; Baluba, S.; Santos, I. C. M. S.; Simoes, M. M. Q.; Graça, M.; Neves, P. M. S.; Cavaleiro, J. A. S.; Cavaleiro, A. M. V. *J. Mol. Catal. A: Chem.* **2004**, *222*, 159−165.
(19) Domaille, P. J.; Harlow, R. L. *J. Am. Chem. Soc.* **1986**, *108*, 2108−2109.
(20) Massiot, D.; Fayon, F.; Capron, M.; King, I.; Calvé, S. Le; Alonso, B.; Durand, J-O.; Bujoli, B.; Gan, Z.; Hoatson, G. *Magn. Reson. Chem.* **2002**, *40*, 70−76.

cation affects only the chemical shift of vanadium sites, contrary to what is observed in Lindqvist-type structures, where the quadrupolar parameters vary also.[8] Indeed, the analysis of the central transition signals of the spectra in Figure 7 demonstrates a small quadrupolar coupling constant, C_Q, for both sites, on the order of 1 MHz, as previously shown for similar structures. The ^{1}H spectrum consists of one narrow resonance at 3.68 ppm (fwhm = 74 Hz) and a second one at 4.56 ppm (fwhm = 1360 Hz). The relative concentration is ca. 76/24. On the basis of the chemical formula $K_3(H_2O)_4[H_2SiV_1W_{11}O_{40}](H_2O)_{8+x,}$ the more-intense band is assigned to the highly mobile hydration water molecules localized in the nanoporous tunnels, in good agreement with the liquid-like sharp peak. The second peak corresponds to the crystalline water molecules that help the cohesion between HPAs. Finally, the single sharp ^{29}Si NMR line (not shown) located at −84.05 ppm is typical of SiO_4 tetrahedra and comforts the structural validity, that is, one independent silicon position.

Conclusion

This work reports the preparation and characterization of the potassium salt of the monosubstituted α-Keggin tungstosilicate $K_3(H_2O)_4[H_2SiVW_{11}O_{40}](H_2O)_{8+x}$. This compound was obtained by the direct addition of sodium vanadate to a solution of the monolacunary α-Keggin polyoxotungstate SiW_{11}. Vibration spectroscopy data confirmed the precipitation of a salt of the nonlacunary α-Keggin polyoxoanion. Single-crystal XRD analysis showed homogeneous distribution of one vanadium atom over the 12 metal positions of the α-Keggin anion. Electronic spectroscopy confirmed the octahedral coordination of vanadium in the compound. Solid-state ^{51}V NMR spectroscopy indicated two vanadium sites in a ratio of 1:2, in agreement with the two different neighborhoods of the V/W sites in the crystal structure. In summary, the analysis clearly shows that vanadium was inserted in the vacant site of the undodecatungstate SiW_{11} species, yielding the monosubstituted $[SiVW_{11}O_{40}]^{5-}$ polyoxoanion. Comparison with the literature suggests that the insertion of vanadium provides stability to the nanoporous-like, Keggin-based crystal structure.

Acknowledgment. We thank CAPES-COFECUB (Grant 436/03) and CNPq for support during this work.

Supporting Information Available: Table of atomic coordinates and equivalent isotropic displacement parameters for $K_3(H_2O)_4[H_2SiVW_{11}O_{40}]\cdot(H_2O)_{6+x}$ and a table of cationic anisotropic displacement parameters in $K_3(H_2O)_4[H_2SiV_1W_{11}O_{40}]\cdot(H_2O)_{8+x}$. This material is available free of charge via the Internet at http://pubs.acs.org.

IC700384M